Spaceborne SAR

Semyon Tsynkov[1]

[1]Department of Mathematics
North Carolina State University, Raleigh, NC

http://www4.ncsu.edu/∼stsynkov/
tsynkov@math.ncsu.edu
+1-919-515-1877

Mathematical and Computational Aspects of Radar Imaging
ICERM, Brown University, October 16–20, 2017

Collaborators and Support

- Collaborators:
  - Dr. Mikhail Gilman (Research Assistant Professor, NCSU)
  - Dr. Erick Smith (Research Mathematician, NRL)
- Support:
  - AFOSR Program in Electromagnetics (Dr. Arje Nachman):
    - ★ Awards number FA9550-14-1-0218 and FA9550-17-1-0230

New research monograph (April 2017)

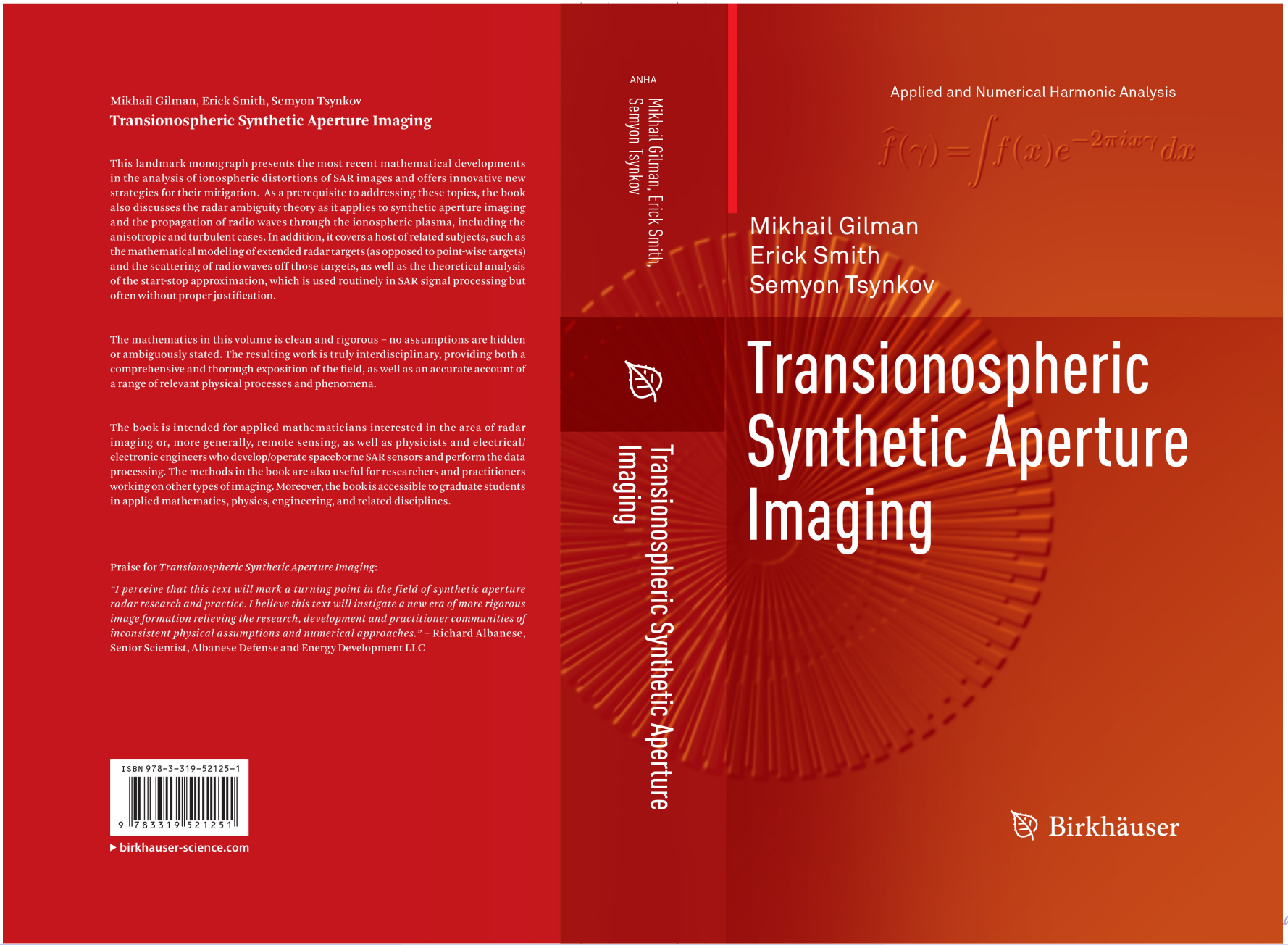

What I plan to accomplish in this talk

- Spaceborne SAR is a vast area:
  - Any attempt to do a broad overview will be superficial.
- Instead, I would like to:
  - Present some recent findings that are unexpected/intriguing;
  - Identify some common misconceptions in the SAR literature.
- Three subjects:
  - Doppler effects and the start-stop approximation;
  - Ionospheric turbulence;
  - Interpretation of targets.

Main idea of SAR

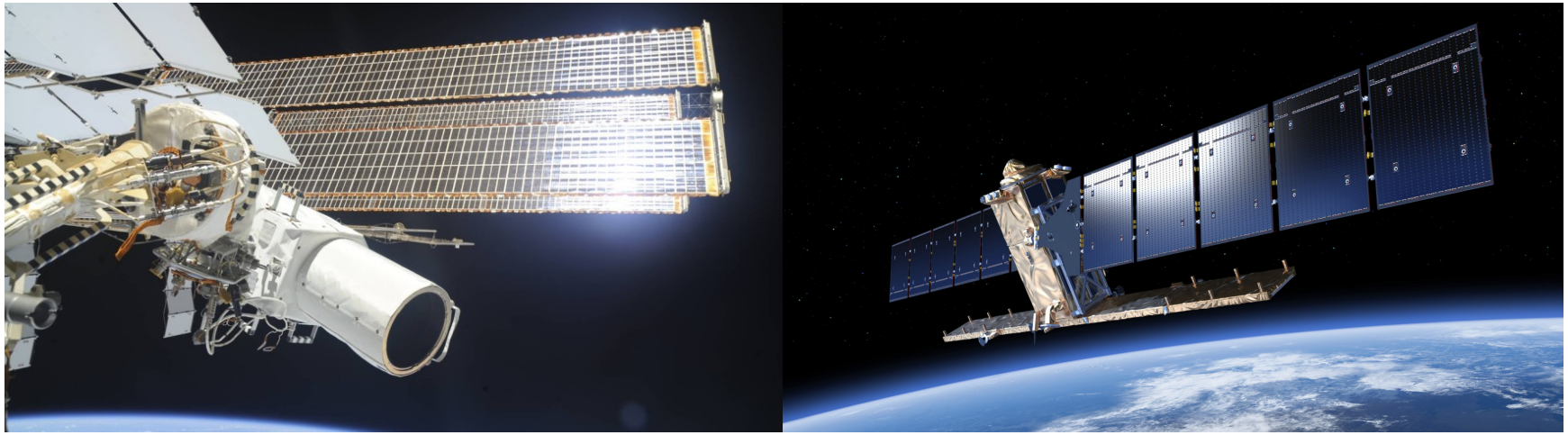

- Coherent overhead imaging by means of microwaves:
  - Typically, P-band to X-band (1 meter to centimeters wavelengh).
- A viable supplement to aerial and space photography.
- To enable imaging, target must be in the near field $\Rightarrow$ instrument size must be very large — unrealistic for actual physical antennas.
- Synthetic array is a set of successive locations of one antenna:
  - Fraunhofer length of the antenna $\frac{2D^2}{\lambda} \ll$ that of the array (aperture);
  - Target in the far field of the antenna is in the near field of the array.

Introduction: monostatic broadside stripmap SAR

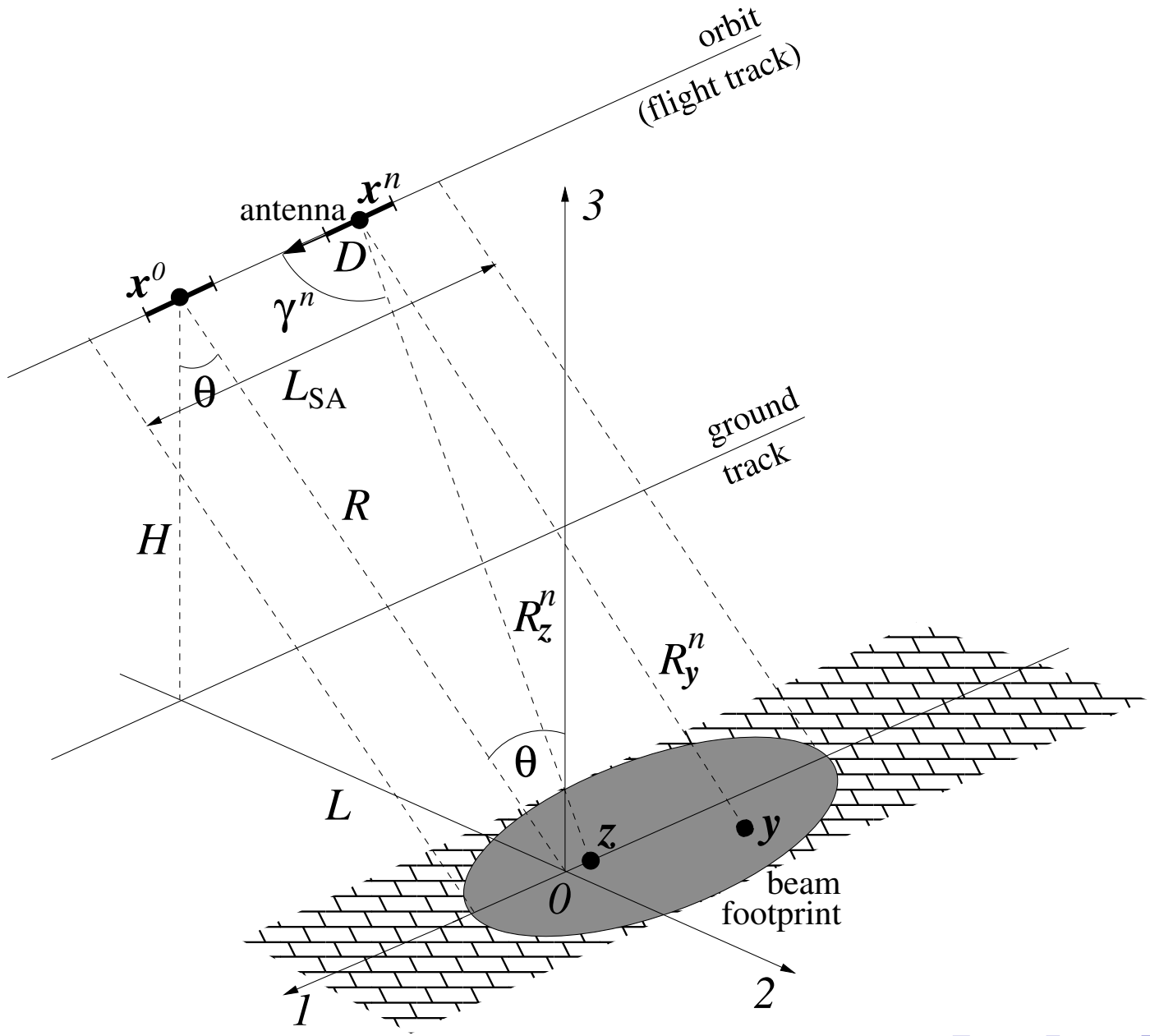

Conventional SAR data inversion

- Interrogating waveforms — linear chirps:

$$P(t) = A(t)e^{-i\omega_0 t}, \quad \text{where} \quad A(t) = \chi_\tau(t)e^{-i\alpha t^2}.$$

- ω_0 — central carrier frequency, τ — duration, $\alpha = \frac{B}{2\tau}$ — chirp rate.
- Incident field — retarded potential from the antenna at $\boldsymbol{x} \in \mathbb{R}^3$:

$$u^{(0)}(t, \boldsymbol{z}) = \frac{1}{4\pi} \frac{P(t - |\boldsymbol{z} - \boldsymbol{x}|/c)}{|\boldsymbol{z} - \boldsymbol{x}|}.$$

- Scattered field for monostatic imaging (ν — ground reflectivity that also "absorbs" the geometric factors):

$$u^{(1)}(t, \boldsymbol{x}) \approx \int \nu(\boldsymbol{z}) P\left(t - 2|\boldsymbol{x} - \boldsymbol{z}|/c\right) d\boldsymbol{z}.$$

  Obtained with the help of the first Born approximation.
- SAR data inversion: reconstruct $\nu(\boldsymbol{z})$ from the given $u^{(1)}(t, \boldsymbol{x})$.
- The inversion is done in two stages:
  - Application of the matched filter (range reconstruction);
  - Summation along the synthetic array (azimuthal reconstruction).

Generalized ambiguity function (GAF)

- Matched filter ($R_y \equiv |\boldsymbol{y}-\boldsymbol{x}|$, $R_z \equiv |\boldsymbol{z}-\boldsymbol{x}|$):

$$I_{\boldsymbol{x}}(\boldsymbol{y}) = \int_{\chi} \overline{P(t-2R_{\boldsymbol{y}}/c)} u^{(1)}(t,\boldsymbol{x})\, dt$$
$$= \int d\boldsymbol{z}\, \nu(\boldsymbol{z}) \underbrace{\int_{\chi} dt\, \overline{P(t-2R_{\boldsymbol{y}}/c)} P(t-2R_{\boldsymbol{z}}/c)}_{W_{\boldsymbol{x}}(\boldsymbol{y},\boldsymbol{z}) \text{ — PSF}}.$$

- Synthetic aperture (determined by the antenna radiation pattern):

$$I(\boldsymbol{y}) = \sum_n I_{\boldsymbol{x}^n}(\boldsymbol{y}) = \sum_n \int W_{\boldsymbol{x}^n}(\boldsymbol{y},\boldsymbol{z})\nu(\boldsymbol{z})d\boldsymbol{z}$$
$$= \int \Big[\sum_n W_{\boldsymbol{x}^n}(\boldsymbol{y},\boldsymbol{z})\Big]\nu(\boldsymbol{z})\, d\boldsymbol{z} = \int W(\boldsymbol{y},\boldsymbol{z})\nu(\boldsymbol{z})\, d\boldsymbol{z} = W * \nu.$$

- $W(\boldsymbol{y},\boldsymbol{z})$ — GAF (or imaging kernel) — convenient for analysis.
  - Actual processing done for the entire dataset rather than for each $\boldsymbol{y}$.

Factorization of the GAF and resolution analysis

- Factorized form of the GAF:

$$W(\boldsymbol{y},\boldsymbol{z}) = W(\boldsymbol{y}-\boldsymbol{z}) \approx \tau \mathrm{sinc}\left(\frac{B}{c}(y_2-z_2)\sin\theta\right) N\mathrm{sinc}\left(\frac{k_0 L_{\mathrm{SA}}}{R}(y_1-z_1)\right).$$

- For narrow-band pulses the factorization error is small: $\mathcal{O}(\frac{B}{\omega_0})$.
- $W(\boldsymbol{y}-\boldsymbol{z}) \neq \delta(\boldsymbol{y}-\boldsymbol{z})$, so the imaging system is not ideal.
- Resolution — semi-width of the main lobe of the sinc$(\,\cdot\,)$:
  - Azimuthal: $\Delta_{\mathrm{A}} = \dfrac{\pi R}{k_0 L_{\mathrm{SA}}} = \dfrac{\pi R c}{\omega_0 L_{\mathrm{SA}}}$; Range: $\Delta_{\mathrm{R}} = \dfrac{\pi c}{B}$.
- What would it be with no phase modulation?
- The range resolution would be $\geqslant$ the length of the pulse τc.
- The actual range resolution is better by a factor of $\dfrac{\tau c}{\Delta_{\mathrm{R}}} = \dfrac{B\tau}{\pi}$.
- $\dfrac{B\tau}{2\pi}$ is the compression ratio of the chirp (or TBP); must be large.

Start-stop approximation and its shortcomings

- The antenna is assumed motionless during the time of emission and reception of a given signal:
  - Then, it moves to the next sending/receiving location.
- This assumption simplifies the analysis yet neglects two important effects:
  - Displacement of the antenna during the pulse round-trip;
  - Doppler frequency shift.
- The corresponding image distortions may be substantial, even though typically $\frac{\mathfrak{v}}{c} \ll 1$.
- Under the start-stop approximation, there may be no physical Doppler effect, because the velocity is considered zero.
  - Yet azimuthal reconstruction is often attributed to the Doppler effect.
  - This is a frequently encountered mistake in the literature.

Schematic for the analysis of antenna motion

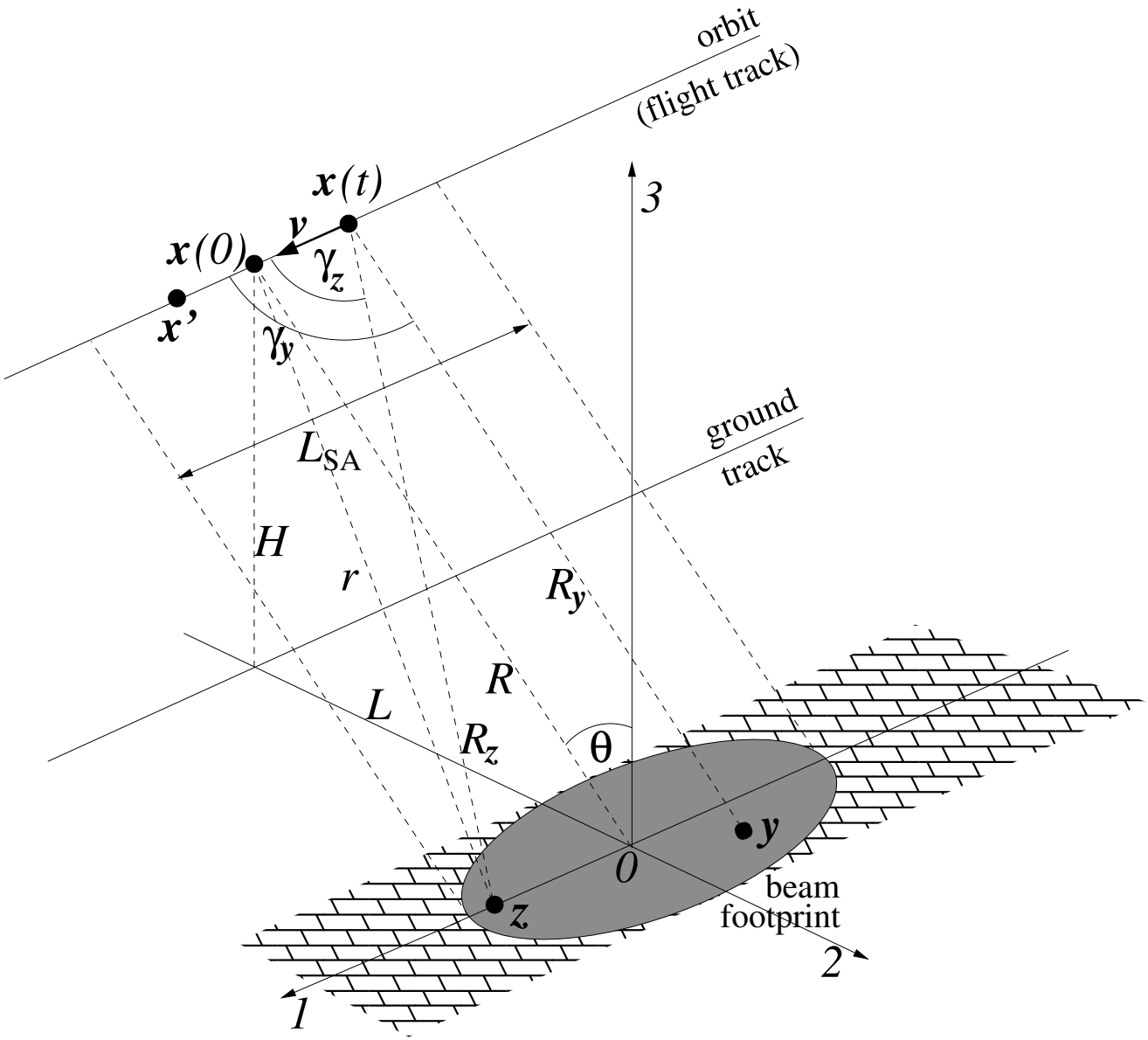

Waves from moving sources

- Analysis uses Lorentz transforms or Liénard-Wiechert potentials.
- Incident field in the original coordinates (where $r = |\boldsymbol{x} - \boldsymbol{z}|$):

$$u^{(0)}(t, \boldsymbol{z}) \approx \frac{1}{4\pi} \frac{P\left(\left(t - \frac{r}{c}\right)\left(1 + \frac{\mathfrak{v}}{c}\cos\gamma_{\boldsymbol{z}}\right)\right)}{r}.$$

- Linear Doppler frequency shift can be obtained by taking $\frac{\partial}{\partial t}$.
- The scattered field in the original coordinates:

$$u^{(1)}(t, \boldsymbol{x}') \approx \int \nu(\boldsymbol{z}) P\left(t\left(1 + 2\frac{\mathfrak{v}}{c}\cos\gamma_{\boldsymbol{z}}\right) - \frac{2r}{c}\left(1 + \frac{\mathfrak{v}}{c}\cos\gamma_{\boldsymbol{z}}\right)\right) d\boldsymbol{z}.$$

- The receiving location $\boldsymbol{x}'$ is not the same as the emitting location $\boldsymbol{x}$.
- Two different factors multiplying the time t and the retarded time $\frac{2r}{c}$.

Data inversion in the presence of antenna motion

- Not a fully relativistic treatment; the terms $\mathcal{O}(\frac{\mathfrak{v}^2}{c^2})$ are neglected.
- Matched filter that accounts for the antenna motion:

$$I_{\boldsymbol{x}}(\boldsymbol{y}) = \int d\boldsymbol{z}\nu(\boldsymbol{z}) \int_{\chi} dt \overline{P\left(t\left(1+2\frac{\mathfrak{v}}{c}\cos\gamma_{\boldsymbol{y}}\right) - \frac{2R_{\boldsymbol{y}}}{c}\left(1+\frac{\mathfrak{v}}{c}\cos\gamma_{\boldsymbol{y}}\right)\right)} \cdot P\left(t\left(1+2\frac{\mathfrak{v}}{c}\cos\gamma_{\boldsymbol{z}}\right) - \frac{2R_{\boldsymbol{z}}}{c}\left(1+\frac{\mathfrak{v}}{c}\cos\gamma_{\boldsymbol{z}}\right)\right).$$

- A simple correction; only geometric info is required.
- Summation along the synthetic array:

$$I(\boldsymbol{y}) = \sum_n I_{\boldsymbol{x}^n}(\boldsymbol{y}) = \sum_n \int W_{\boldsymbol{x}^n}(\boldsymbol{y},\boldsymbol{z})\nu(\boldsymbol{z})d\boldsymbol{z}$$
$$= \int \Big[\sum_n W_{\boldsymbol{x}^n}(\boldsymbol{y},\boldsymbol{z})\Big]\nu(\boldsymbol{z})\,d\boldsymbol{z} = \int W(\boldsymbol{y},\boldsymbol{z})\nu(\boldsymbol{z})\,d\boldsymbol{z} = W * \nu.$$

The GAF in the presence of antenna motion

- The azimuthal factor:

$$W_{\mathrm{A}}(\boldsymbol{y},\boldsymbol{z}) \approx N\mathrm{sinc}\left(\frac{k_0 L_{\mathrm{SA}}}{R}\left(\underbrace{(y_1-z_1)}_{\text{original}}+\underbrace{2\frac{L(y_2-z_2)}{R}\frac{\mathfrak{v}}{c}}_{\text{due to Doppler}}\right)\right).$$

- The range factor:

$$W_{\mathrm{R}}(\boldsymbol{y},\boldsymbol{z}) \approx \tau\mathrm{sinc}\left(\frac{B}{c}\left(\underbrace{(y_2-z_2)\sin\theta}_{\text{original}}-\underbrace{(y_1-z_1)\frac{\mathfrak{v}}{c}\overbrace{\left(1+\frac{\omega_0}{\alpha R}\frac{c}{2}\right)}^{\text{typically } \mathcal{O}(1)}}_{\text{due to Doppler}}\right)\right).$$

- "Cross-contamination" is small; the resolution remains unaffected.
- Factorization error is still $\mathcal{O}(\frac{B}{\omega_0})$:

$$\frac{\max|W-W_{\mathrm{R}}W_{\mathrm{A}}|}{\max|W_{\mathrm{R}}W_{\mathrm{A}}|} \lesssim \frac{B}{8\omega_0}\frac{\pi}{\Delta_{\mathrm{A}}}\left|(y_1-z_1)+\frac{L(y_2-z_2)}{R}\frac{\mathfrak{v}}{c}\left(4+\frac{\omega_0 c}{2\alpha R}\right)\right|.$$

SAR with no filter correction: the real start-stop

- Plain non-corrected filter applied to Doppler-based propagator:

$$I_{\boldsymbol{x}}(\boldsymbol{y}) = \int d\boldsymbol{z}\nu(\boldsymbol{z}) \int_{\chi} dt \overline{P\left(t - \frac{2R_{\boldsymbol{y}}}{c}\right)} \cdot P\left(t\left(1 + 2\frac{\mathfrak{v}}{c}\cos\gamma_{\boldsymbol{z}}\right) - \frac{2R_{\boldsymbol{z}}}{c}\left(1 + \frac{\mathfrak{v}}{c}\cos\gamma_{\boldsymbol{z}}\right)\right).$$

- The factors W_{R} and W_{A} change insignificantly. Yet they cannot be directly used for resolution analysis due to the factorization error:

$$\frac{\max|W - W_{\mathrm{R}}W_{\mathrm{A}}|}{\max|W_{\mathrm{R}}W_{\mathrm{A}}|} \lesssim \frac{B}{8\omega_0}\frac{\pi}{\Delta_{\mathrm{A}}}\left|(y_1 - z_1) + \frac{\mathfrak{v}}{c}R\left(1 + \frac{\omega_0}{\alpha R}\frac{c}{2}\right)\right|.$$

- The term $\frac{\omega_0}{\alpha R}\frac{c}{2}$ may become large if, e.g., α is small.
- Ignoring this error may seriously underestimate image distortions:
  - FMCW SAR may be particularly prone to deterioration.

ViSAR project by DARPA

- A SAR instrument to operate in the EHF band (at 235GHz).
- FMCW interrogating waveforms due to hardware limitations:
  - FMCW = Frequency Modulated Continuous Wave.

Doppler interpretation of azimuthal reconstruction

- Azimuthal reconstruction is often erroneously attributed to the physical Doppler effect, which does not exist under start-stop.
- Can one think of a meaningful counterpart?
- Linear variation of the instantaneous frequency along the chirp $2\alpha t = \omega(t) - \omega_0$ yields the range factor of the GAF:

$$W_{\mathrm{R}}(\boldsymbol{y}, \boldsymbol{z}) = \int_{\chi} e^{-i\alpha 4t(R^{\mathrm{c}}_{\boldsymbol{y}} - R^{\mathrm{c}}_{\boldsymbol{z}})/c} dt = \int_{\chi} e^{-2i(\omega(t)-\omega_0)(R^{\mathrm{c}}_{\boldsymbol{y}} - R^{\mathrm{c}}_{\boldsymbol{z}})/c} dt.$$

- In the azimuthal factor, there is a linear variation of the local wavenumber along the array, $k(n) = k_0 \dfrac{L_{\mathrm{SA}} n}{RN}$:

$$W_{\mathrm{A}}(\boldsymbol{y}, \boldsymbol{z}) = \sum_n e^{2ik_0 \frac{L_{\mathrm{SA}} n}{RN}(y_1 - z_1)} = \sum_n e^{2ik(n)(y_1 - z_1)}.$$

- Can be thought of as a chirp of length L_{SA} in azimuth.

Doppler effect in slow time

- The instantaneous wavenumber $k(n)$ can be transformed as

$$k(n) = -k_0 \cos \frac{\gamma_{\boldsymbol{y}}^n + \gamma_{\boldsymbol{z}}^n}{2} \stackrel{\text{def}}{=} -k_0 \cos \tilde{\gamma}^n.$$

- This is similar to the physical Doppler effect:

$$\omega - \omega_0 = \omega_0 \frac{\mathfrak{v}}{c} \cos \gamma.$$

- Hence, the linear variation of $k(n)$ can be attributed to a Doppler effect in slow time n, and we can write:

$$W_{\text{A}}(\boldsymbol{y}, \boldsymbol{z}) = \sum\nolimits_n e^{-2ik_0 \cos \tilde{\gamma}^n (y_1 - z_1)} = \sum\nolimits_n e^{-2i\omega_0 \cos \tilde{\gamma}^n (y_1 - z_1)/c}.$$

- There is no velocity factor in the slow time Doppler effect, because everything can be thought of as taking place simultaneously.
- The geometric factor $\cos \tilde{\gamma}^n$ is basically the same as that from the physical Doppler effect (or the Doppler effect in fast time).

Signal compression in the azimuthal direction

- Compression ratio (or TBP) of the actual chirp is the ratio of its length to the range resolution:

$$\frac{\tau c}{\Delta_{\mathrm{R}}} = \frac{B\tau}{\pi} \gg 1.$$

  It quantifies the improvement due to phase modulation.
- For the chirp in the azimuthal direction we have:

$$\frac{L_{\mathrm{SA}}}{\Delta_{\mathrm{A}}} = \frac{2L_{\mathrm{SA}}^2}{\lambda_0}\frac{1}{R} \gg 1,$$

  where $\lambda_0 = \frac{2\pi c}{\omega_0}$ is the central carrier wavelength.
- Why is this quantity (azimuthal compression ratio) $\gg 1$?
- Because $\frac{2L_{\mathrm{SA}}^2}{\lambda_0}$ is the Fraunhofer distance of the synthetic array.

Ionospheric distortions of SAR images

- EM waves in the ionosphere are subject to temporal dispersion:
  - $v_{\rm gr} < c$ — group delay;
  - $v_{\rm ph} > c$ — phase advance;
  - The duration τ of the chirp and its rate α change.
- Mismatch between the received signal and the matched filter.
- Can be reduced by adjusting the filter — real-time TEC/gradients needed — can be obtained with the help of dual carrier probing:
  - Correction is more involved than in the case of Doppler;
  - Correction is efficient if the moments don't vary over the image.
- However, the ionosphere is a turbulent medium.
- Synthetic aperture may be comparable to the scale of turbulence.
- Parameters of the medium will fluctuate from one pulse to another:
  - Using a single correction may still leave room for mismatches.
- One needs to quantify the image distortions due to turbulence:
  - How can one "marry" the deterministic and random errors?

Monostatic broadside stripmap SAR

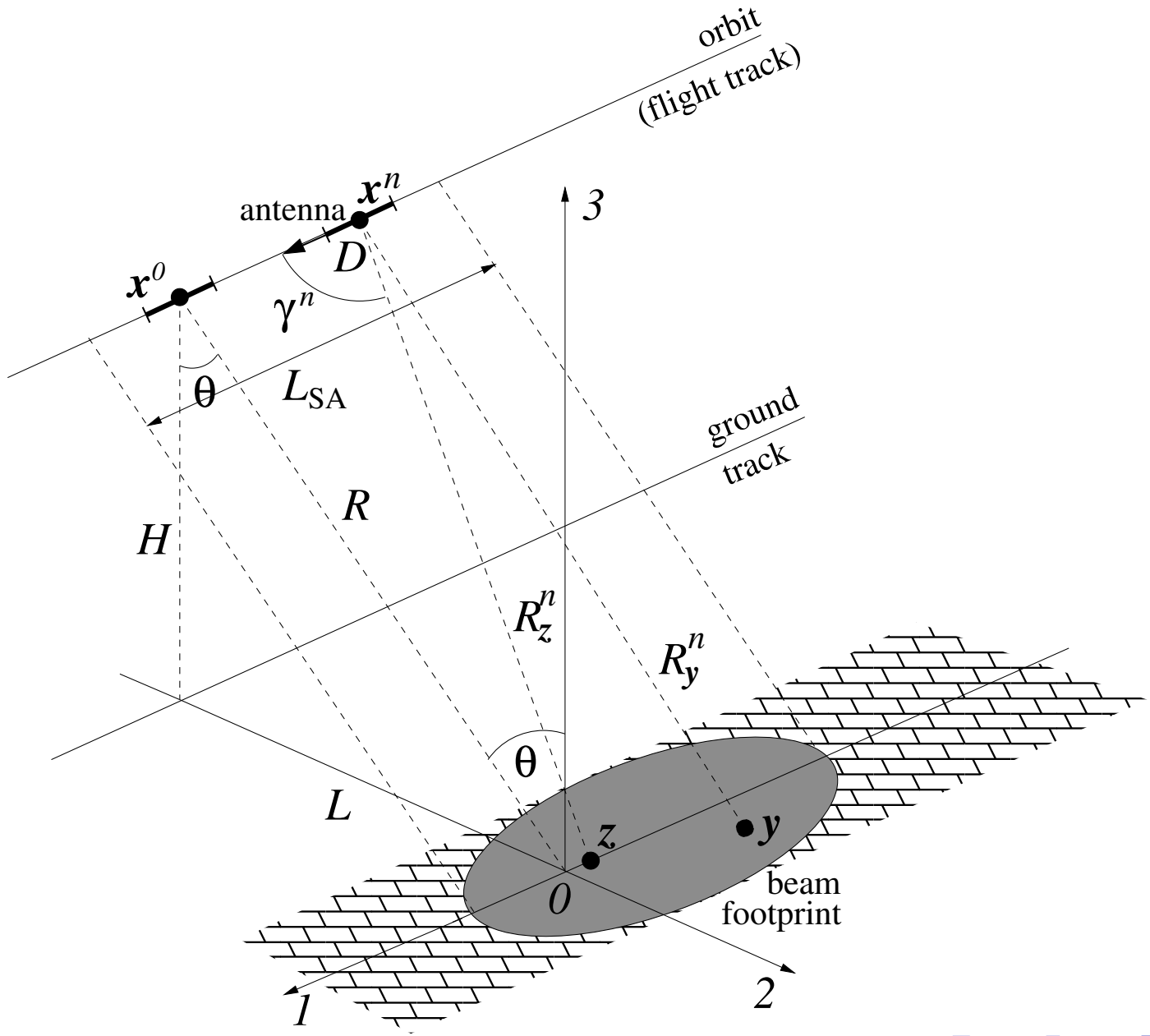

Recalling the math of transionospheric SAR

- Convolution representation of the image (requires linearity):

$$I(\boldsymbol{y}) = \int \nu(\boldsymbol{z}) W(\boldsymbol{y}, \boldsymbol{z}) d\boldsymbol{z}.$$

- The imaging kernel (or GAF — generalized ambiguity function):

$$W(\boldsymbol{y}, \boldsymbol{z}) = \sum_n e^{-2i\omega_0 T^n_{\mathrm{ph}}} \int_{-\tau/2}^{\tau/2} e^{-4i\tilde{\alpha}^n T^n_{\mathrm{gr}} t} dt,$$

where $T^n_{\mathrm{ph,\,gr}} = T_{\mathrm{ph,\,gr}}(\boldsymbol{x}^n, \boldsymbol{y}, \omega_0) - T_{\mathrm{ph,\,gr}}(\boldsymbol{x}^n, \boldsymbol{z}, \omega_0)$ and

$$T_{\mathrm{ph,\,gr}}(\boldsymbol{x}, \boldsymbol{z}, \omega_0) = \int_0^{R_{\boldsymbol{z}}} \frac{1}{v_{\mathrm{ph,\,gr}}(s)} ds \approx \int_0^{R_{\boldsymbol{z}}} \frac{1}{c}\left(1 \mp \frac{1}{2}\frac{4\pi e^2}{m_{\mathrm{e}}\omega_0^2} N_{\mathrm{e}}(s)\right) ds = \frac{R_{\boldsymbol{z}}}{\bar{v}_{\mathrm{ph,\,gr}}}.$$

- Factorization:

$$W(\boldsymbol{y}, \boldsymbol{z}) \approx \tau N \mathrm{sinc}\left(\frac{B(y_2 - z_2)\sin\theta}{\bar{v}_{\mathrm{gr}}}\right) \mathrm{sinc}\left(\frac{\omega_0 (y_1 - z_1) L_{\mathrm{SA}}}{R\,\bar{v}_{\mathrm{ph}}}\right).$$

In the presence of turbulence

- The electron number density: $N_{\mathrm{e}} = \langle N_{\mathrm{e}} \rangle + \mu(\boldsymbol{x}), \quad \langle \mu \rangle = 0.$
- The travel times become random:

$$T_{\mathrm{ph,\,gr}}(\boldsymbol{x}, \boldsymbol{z}, \omega_0) = \frac{R_{\boldsymbol{z}}}{\bar{v}_{\mathrm{ph,\,gr}}} \mp \frac{1}{2c} \frac{4\pi e^2}{m_{\mathrm{e}} \omega_0^2} \int_0^{R_{\boldsymbol{z}}} \mu(\boldsymbol{x}(s)) ds \equiv \frac{R_{\boldsymbol{z}}}{\bar{v}_{\mathrm{ph,\,gr}}} \mp \frac{\varphi}{2c}.$$

- Accordingly, the GAF also becomes random (stochastic):

$$W'(\boldsymbol{y}, \boldsymbol{z}) = \sum_n e^{-2i\omega_0 T'^n_{\mathrm{ph}}} \int_{-\tau/2}^{\tau/2} e^{-4i\alpha T'^n_{\mathrm{gr}} t} dt,$$

where

$$T'^n_{\mathrm{ph,\,gr}} = \frac{R^n_{\boldsymbol{y}}}{\bar{v}_{\mathrm{ph,\,gr}}} - T_{\mathrm{ph,\,gr}}(\boldsymbol{x}^n, \boldsymbol{z}, \omega_0) = \frac{R^n_{\boldsymbol{y}} - R^n_{\boldsymbol{z}}}{\bar{v}_{\mathrm{ph,gr}}} \pm \frac{\varphi_n}{2c}.$$

Statistics of propagation

- Correlation function of the medium (turbulent fluctuations):

$$V(\boldsymbol{x}', \boldsymbol{x}'') \stackrel{\text{def}}{=} \left\langle \mu(\boldsymbol{x}')\mu(\boldsymbol{x}'') \right\rangle = \langle \mu^2 \rangle V_r(r) = M^2 \langle N_{\text{e}} \rangle^2 V_r(r),$$

  where $V_r(r) \equiv V_r(|\boldsymbol{x}' - \boldsymbol{x}''|)$ decays rapidly, e.g., $V_r(r) = e^{-r/r_0}$.
- Other short-range correlation functions include Gaussian and Kolmogorov-Obukhov.
- Correlation radius of the medium (outer scale of turbulence):

$$r_0 \stackrel{\text{def}}{=} \frac{1}{V_r(0)} \int_0^\infty V_r(r) dr.$$

- Variance of the eikonal quantifies the magnitude of phase fluctuations:

$$\left\langle \varphi^2 \right\rangle = \left(\frac{4\pi e^2}{m_{\text{e}} \omega_0^2} \right)^2 M^2 \int_0^{R_{\boldsymbol{z}}} \left\langle N_{\text{e}}(h(s)) \right\rangle^2 ds \cdot 2 \int_0^\infty V_r(r)\, dr.$$

- Covariance of the eikonal is of central importance: $\left\langle \varphi_m \varphi_n \right\rangle$.

Covariance of the eikonal (phase path)

- Affected by statistics of the medium and propagation geometry:

$$\langle \varphi_m \varphi_n \rangle = \left(\frac{4\pi e^2}{m_e \omega_0^2} \right)^2 RM^2 \int_0^1 d\mathfrak{u} \, \langle N_e(h(\mathfrak{u}R)) \rangle^2 \int_{-\infty}^{\infty} ds V_r\left(\sqrt{\mathfrak{u}^2 |\boldsymbol{x}_m - \boldsymbol{x}_n|^2 + s^2} \right).$$

- A common misconception: not accounting for the ionopause.

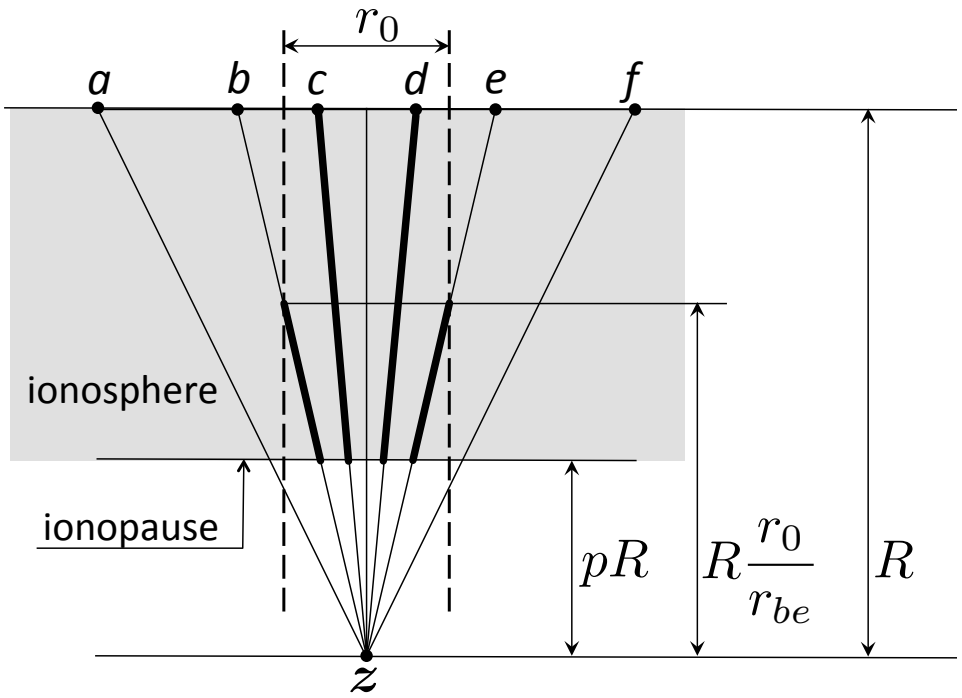

- With no ionopause, $\langle \varphi_m \varphi_n \rangle$ decays slowly even if the correlation function of the medium is short-range.
- With the ionopause, $\langle \varphi_m \varphi_n \rangle$ is also short-range (like V_r) and $r_\varphi \sim r_0$.
- Why is $\langle \varphi_m \varphi_n \rangle$ important?

Stochastic GAF

- Factorization:

$$W'(\boldsymbol{y},\boldsymbol{z}) \approx \tau \text{sinc}\left(\frac{B(y_2 - z_2)\sin\theta}{\bar{v}_{\text{gr}}}\right) \cdot \sum_n e^{-2i\omega_0 T'^n_{\text{ph}}}$$

- For narrow-band signals, the factorization error is small: $\mathcal{O}(\frac{B}{\omega_0})$.
- The effect of turbulence on the imaging in range can be shown to be negligibly small compared to its effect on imaging in azimuth.
- What remains is the sum of random variables over the array.
- Why is it important to know how rapidly the random phase decorrelates along the array?
  - Random phases are normal due to the central limit theorem.
  - Terms in the sum are log-normal: Uncorrelated $\Leftrightarrow$ Independent.
- Statistical dependence or independence of the constituent terms directly affect the moments of the stochastic GAF.

Errors due to randomness

- The mean of the stochastic GAF reduces to the deterministic GAF (subject to extinction $\propto e^{-\pi\langle\varphi^2\rangle/\lambda_0^2}$):
  - The deterministic errors include plain SAR, ionosphere, Doppler...
- The errors due to randomness are superimposed on the above:
  - When $r_\varphi \ll L_{\mathrm{SA}}$ and $\sqrt{\langle\varphi^2\rangle} \ll \lambda_0$ (small-scale turbulence with small fluctuations), they are estimated by variance of the stochastic GAF:

$$\sqrt{\sigma^2_{W'_{\mathrm{A}}}} = \sqrt{2}\frac{\omega_0}{c} N \sqrt{\frac{\langle\varphi^2\rangle}{L_{\mathrm{SA}}/r_\varphi}}$$

  - $\sigma^2_{W'_{\mathrm{A}}}$ quantifies the difference between stochastic and deterministic GAF and accounts for the variation within the statistical ensemble.
- Yet mechanically adding the two types of errors may be ill-advised:
  - In reality, there is a single image rather than an ensemble;
  - For $r_\varphi \ll L_{\mathrm{SA}}$, randomness manifests itself within a single image;
  - For $r_\varphi \gg L_{\mathrm{SA}}$, random phases φ_n within the array are identical:
    - ★ $\sqrt{\sigma^2_{W'_{\mathrm{A}}}}$ is large, yet it basically becomes irrelevant.

Errors due to randomness (cont'd)

- The case $r_\varphi \gg L_{\mathrm{SA}}$ is very similar to fully deterministic:
  - Image distortions due to randomness can be characterized directly in terms of the azimuthal shift and blurring (expected values),
    - ⋆ NOT as the difference between the stochastic and deterministic GAF;
  - Blurring is significant only for much larger fluctuations than the shift:
    - ⋆ One can have a shifted yet otherwise decent (low blurring) image even for $\sqrt{\langle \varphi^2 \rangle} \gg \lambda_0$.
- On the other hand, in the case $r_\varphi \ll L_{\mathrm{SA}}$, $\sqrt{\langle \varphi^2 \rangle} \gg \lambda_0$ (small-scale turbulence with large fluctuations), the image is completely destroyed [Garnier & Solna, 2013].
- No "continuous transition" (yet) between the small-scale case and large-scale case.
- Correction of image distortions due to turbulence is a major issue:
  - Current analysis is aimed only at quantification of distortions.

Why do we need new models for radar targets?

- The image $I(\boldsymbol{y})$ is a convolution-type integral:

$$I(\boldsymbol{y}) = \int \nu(\boldsymbol{z}) W(\boldsymbol{y}, \boldsymbol{z}) d\boldsymbol{z},$$

  where ν characterizes the target, and W — the imaging system.
- The reflectivity $\nu(\boldsymbol{z})$ is either phenomenological or physics-based.
- Scattering must be linear with respect to the target properties ν:
  - $\nu(\boldsymbol{z})$ is proportional to the variation of the local refractive index;
  - Assumption: Weak scattering $\Leftrightarrow$ the first Born approximation.
- Scattering occurs only at the surface of the target; $d\boldsymbol{z} = dz_1 dz_2$.
  - Why? — microwaves do not penetrate under the surface.
- Weak scattering is inconsistent with no-penetration conjecture.
- A flat uniform target won't backscatter...
  - What is the actual observable quantity in SAR?
  - How is it related to the local properties of the scatterer?

Scattering about a dielectric half-space

- Scattering off a material half-space with a planar interface:

$$n^2(\boldsymbol{z}) = \varepsilon(\boldsymbol{z}) = \begin{cases} 1, & z_3 > 0, \\ \varepsilon^{(0)} + \varepsilon^{(1)}(z_1, z_2), & z_3 < 0, \end{cases}$$

  where $|\varepsilon^{(1)}| \ll \varepsilon^{(0)} = \text{const}$. The background permittivity $\varepsilon^{(0)}$ can be large, so the scattering is not necessarily weak.

- The method of perturbations:

$$u(t, \boldsymbol{z}) = u^{(0)}(t, \boldsymbol{z}) + u^{(1)}(t, \boldsymbol{z}),$$

  where $|u^{(1)}| \ll |u^{(0)}|$.

- Linearization: higher order terms $\sim \varepsilon^{(1)} u^{(1)}$ are dropped.

Schematic for the scattering geometry

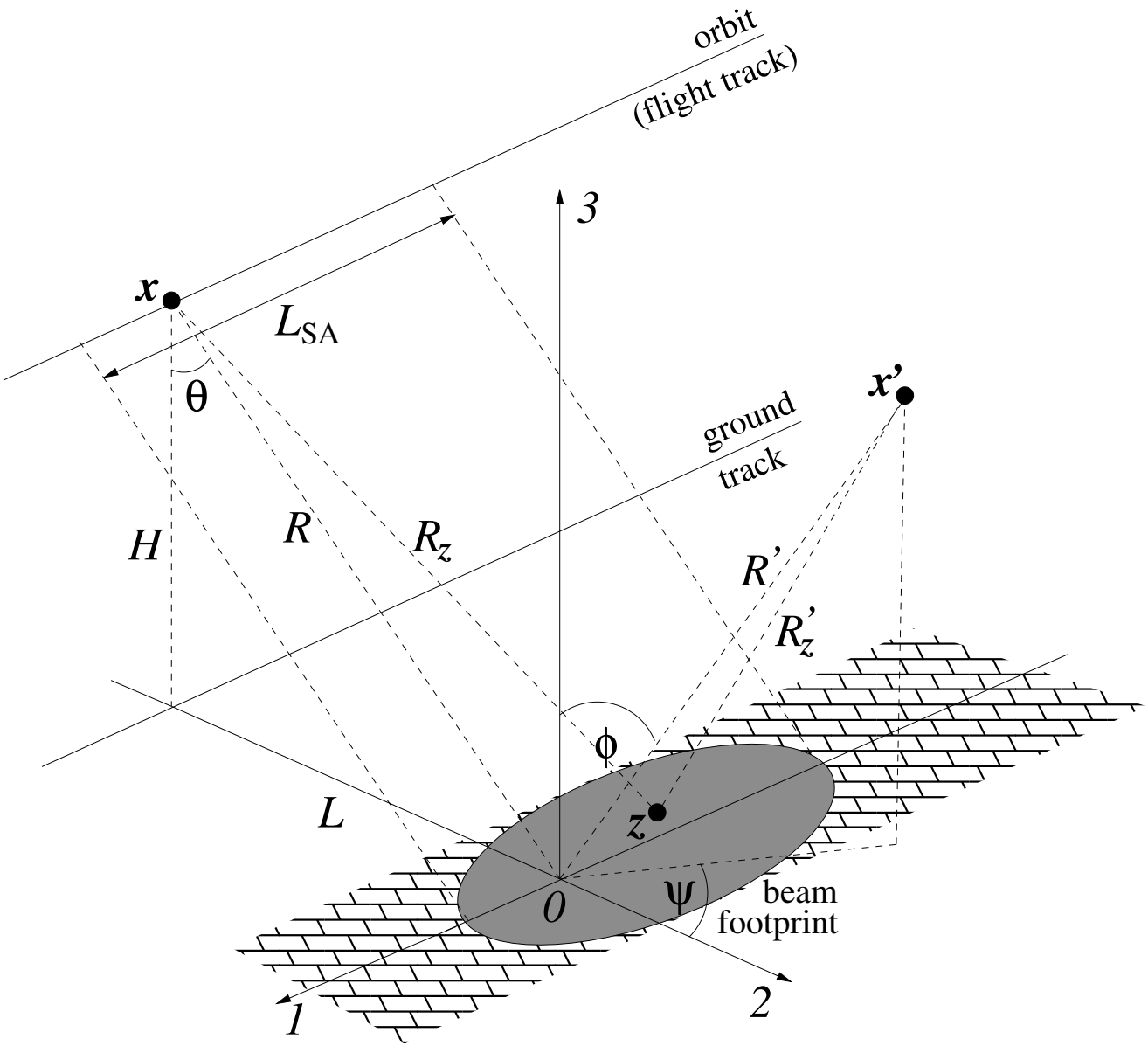

Solution for the scattered field

- The field is governed by the wave (d'Alembert) equation:

$$\left(\frac{n^2}{c^2}\frac{\partial^2}{\partial t^2} - \Delta\right)(u^{(0)} + u^{(1)}) = 0.$$

- The field and its normal derivative are continuous at the interface.
  - Interface conditions hold separately for the zeroth and first order.
- Zeroth order solution by Fresnel formulae.
  - May involve strong refraction.
- First order solution using the separation of variables rendered by Fourier transform in time t and along the surface (z_1, z_2).
- Uncoupled ODEs in the direction z_3 are solved in closed form.
- The inverse transform is done by stationary phase; it accounts for any reflection angles ϕ and ψ if the distance to the surface is large.

Surface retarded potential

- Scattered field in the time domain:

$$u^{(1)}(t,\boldsymbol{x}') = \frac{\mathcal{M}(\varepsilon^{(0)},\theta,\phi)}{4\pi^2 RR'c}\iint P'\left(t-\frac{R_{\boldsymbol{z}}+R'_{\boldsymbol{z}}}{c}\right)\varepsilon^{(1)}(z_1,z_2)dz_1dz_2,$$

  where

$$\mathcal{M} = \frac{\cos\theta\cos\phi}{\left(\cos\phi+\sqrt{\varepsilon^{(0)}-\sin^2\phi}\right)\left(\sqrt{\varepsilon^{(0)}-\sin^2\phi}+\sqrt{\varepsilon^{(0)}-\sin^2\theta}\right)\left(\cos\theta+\sqrt{\varepsilon^{(0)}-\sin^2\theta}\right)}.$$

- It is a surface retarded potential obtained with no inconsistent assumptions and no use of the first Born approximation:
  - Convolutions are two-dimensional by design;
  - The scattering is linear yet not necessarily weak.
- For backscattering ($\boldsymbol{x}=\boldsymbol{x}'$), the previous expression simplifies:

$$u^{(1)}(t,\boldsymbol{x}) = \frac{\mathcal{M}(\varepsilon^{(0)},\theta,\theta)}{4\pi^2 R^2 c}\iint P'\left(t-2\frac{R_{\boldsymbol{z}}}{c}\right)\varepsilon^{(1)}(z_1,z_2)dz_1dz_2.$$

What is the SAR observable quantity?

- The reflection coefficient for monostatic imaging (as $P' \approx -i\omega_0 P$):

$$\nu(z_1, z_2) = -i\omega_0 \frac{\mathcal{M}(\varepsilon^{(0)}, \theta, \theta)}{4\pi^2 R^2 c} \varepsilon^{(1)}(z_1, z_2).$$

- Yet is it the reflectivity $\nu(z_1, z_2)$ itself that we actually see?
- The scattered field is given by "almost" the Fourier transform at the Bragg frequency $k_\theta = -2k_0 \sin\theta$ (R_z is linearized):

$$\begin{aligned} u^{(1)}(t, \boldsymbol{x}) &\approx -i\omega_0 \frac{\mathcal{M}(\varepsilon^{(0)}, \theta, \theta)}{4\pi^2 R^2 c} \iint P\Big(t - 2\frac{R_z}{c}\Big) \varepsilon^{(1)}(z_1, z_2) dz_1 dz_2 \\ &\propto -i\omega_0 \frac{\mathcal{M}(\varepsilon^{(0)}, \theta, \theta)}{4\pi^2 R^2 c} \iint A\Big(t - 2\frac{R_z}{c}\Big) e^{2ik_0 z_2 \sin\theta} \varepsilon^{(1)}(z_1, z_2) dz_2 dz_1. \end{aligned}$$

- The true mechanism of surface scattering is resonant.
- If $\nu(z_1, z_2)$ has no spectral content at or around k_θ, then there is no backscattering, and no monostatic SAR image can be obtained.

Physical interpretation of SAR observables

- The image:

$$I(\boldsymbol{y}) = \int dz_1 \int dz_2 \; W_{\mathsf{A}}(y_1, z_1) W_{\mathsf{R}}(y_2, z_2) \nu^{\mathsf{new}}(z_1, z_2).$$

- ν^{new} is obtained by shifting and band limiting the spectrum of ν:

$$\hat{\nu}^{\mathsf{new}}(z_1, k) = \hat{\nu}(z_1, k + k_\theta) \chi_\beta(k),$$

  where $k_\theta = -2k_0 \sin\theta$ is the Bragg frequency, and $\beta = \frac{2B \sin\theta}{c}$.
- ν^{new} varies slowly in space, on the scale $\gtrsim \Delta_{\mathsf{R}} = \frac{\pi c}{B}$, because all its spatial frequencies $\leqslant \frac{\beta}{2} \ll |k_\theta| \Leftrightarrow B/c \ll k_0$ or $B \ll \omega_0$.
- Alternatively, the observable quantity $\nu^{\mathsf{new}}(z_1, z_2)$ can be derived as a window Fourier transform (WFT) of ν:

$$\nu^{\mathsf{new}}(z_1, z_2) = \frac{\tau \sin\theta}{\Delta_{\mathsf{R}}} \int W_{\mathsf{R}}(z_2 - z') \nu(z_1, z') e^{-ik_\theta z'} dz'.$$

- $\nu^{\mathsf{new}}(z_1, z_2)$ is a slowly varying amplitude of the Bragg harmonic $e^{ik_\theta z_2}$ in the spectrum of ν computed on a Δ_{R} size sinc $(\cdot)$ window.

What does it mean for imaging?

- The actual quantity reconstructed by SAR is not the reflectivity per se but rather its particular slowly varying spectral component.
  - Yet the reconstruction itself is enabled by the presence of high frequencies.
- Implications for angular coherence in the case of wide apertures:
  - The WFT along different directions for different antenna positions.
- Vector extension is possible that would account for polarization.
- Anisotropic and/or lossy materials can be considered.
- Other models include Leontovich and rough surface.

Thank you for your attention!